

1 **Facultative commensalism of free-burrowing, urothoid amphipod with deep burrow-dwelling**  
2 **callianassid shrimp on an intertidal sandflat**

3

4 Akio Tamaki<sup>1,\*</sup>, Takumi Kagesawa<sup>2</sup>, Seiji Takeuchi<sup>1</sup>, Hirofumi Ohashi<sup>2</sup>, Soonbo Yang<sup>3</sup>, Shinji  
5 Sassa<sup>3</sup>

6

7 1) Graduate School of Fisheries and Environmental Sciences, Nagasaki University, Bunkyo-machi  
8 1-14, Nagasaki 852-8521, Japan

9 2) Faculty of Fisheries, Nagasaki University, Nagasaki 852-8521, Japan

10 3) National Research and Development Agency, National Institute of Maritime, Port and Aviation  
11 Technology, Port and Airport Research Institute, Yokosuka 239-0826, Japan

12

13 \*) Corresponding author e-mail: tamaki@nagasaki-u.ac.jp; telephone: +81-95-819-2856

14

15

16

17

18

19

20

21

22

23

24

25 **Abstract**

26 Species of the free-burrowing amphipod genus, *Urothoe*, are common macrobenthos on open sandy  
27 beaches. On intertidal sandflats, some species are associated with burrows or tubes of large infauna.  
28 How this link is formed under sheltered settings was examined. On an intertidal sandflat emerged for  
29 300 m seaward in mid-western Kyushu, Japan, *U. carda* co-occurred with the deep burrow-dwelling  
30 callianassid shrimp, *Nihonotrypaea harmandi*. Amphipods resided in the surface 5-cm sediment  
31 outside shrimp burrows, as confirmed by sediment coring and burrow casting. In the summertime  
32 during 1980 to 1981, the shrimp and amphipod populations were confined to the upper shore at  
33 mean densities of 182 and 701 inds m<sup>-2</sup>, respectively. In winter to spring, when the sediment surface  
34 mixing was caused by seasonal wind-induced waves, only the amphipod extended distribution to the  
35 lowest shore. By 1983, the shrimp increased mean density by 2.5 times and distribution range to the  
36 lowest shore. In the summers of 1984, 2010, and 2015, the amphipod extended distribution to the  
37 lowest shore, with small variations in population size. Three marked changes in substrate properties  
38 were associated with the shrimp inhabitation: thicker oxidized layer (proxy for oxygenated layer) in  
39 the sediment column; looser surface sediment, as evaluated with vane shear strength; and coarser  
40 and better-sorted surface sediment with less mud content. At least the former two changes were  
41 attributable to shrimp bioturbation, which could provide the amphipod with more permeable and  
42 softer substrates, leading to the formation of facultative commensalism.

43

44 **Introduction**

45 Species of the gammaridean amphipod genus, *Urothoe*, are cosmopolitan members of the benthic  
46 macro-infauna on open sandy beaches and shallow subtidal sandy bottoms (Bousfield 1970; Bally  
47 1983; Barnard and Karaman 1991). Their high burrowing ability is an adaptation to shifting  
48 sediment, with broad-fusiform body form believed suited to filter-feeding in loosely packed sand

49 (Bousfield 1970). Among the free-burrowing amphipods, adults of *Urothoe* spp. reside relatively  
50 deep in the sediment (Vader 1978; Sudo 1988). *Urothoe* spp. also occur as surf plankton (Fincham  
51 1970; Yu et al. 2002), with males performing nocturnal excursions into the water column probably as  
52 a part of mating behavior (Fincham 1970; Sudo 1988; Fernandez-Gonzalez et al. 2014). Some  
53 species of *Urothoe* inhabit intertidal sandflats that are more sheltered than open sandy beaches. On  
54 sheltered habitats, individuals of some *Urothoe* spp. are associated with deep burrows or tubes of  
55 much larger-bodied infauna such as ophiuroids, spatangoid echinoids, and an apodid holothuroid  
56 (Vader 1978), an arenicolid polychaete (Lackschewitz and Reise 1998), and a terebellid polychaete  
57 (Callaway 2006). Individuals of these *Urothoe* spp. dwell inside (Vader 1978; Lackschewitz and  
58 Reise 1998) and/or closely outside (Vader 1978; Lackschewitz and Reise 1998; Callaway 2006) the  
59 deeper part of those macrobenthos' burrows or tubes. Steady oxygen and/or food supply around the  
60 large polychaete burrows or tubes were suggested to be attractive to *U. poseidonis* (see  
61 Lackschewitz and Reise 1998; Callaway 2006). How and to what degree such *Urothoe* spp. co-occur  
62 with their presumed hosts under sheltered settings remain to be elucidated.

63 In a survey for the density and distribution of macrofauna on an intertidal sandflat in mid-  
64 western Kyushu, Japan (Tomioka sandflat; Fig. 1) conducted in the summer of 1979, *Urothoe carda*  
65 was the eighth numerically dominant species of a total of 58 species of the benthic community  
66 [Tamaki and Kikuchi (1983), with the name, *U. grimaldii*, incorrectly used; total length range:  
67 0.8–5.3 mm (A. Tamaki et al., unpubl data)]. The population of *U. carda* occurred mainly in a zone  
68 quasi-parallel to the shoreline densely inhabited by the callianassid decapod shrimp (or ghost  
69 shrimp), *Nihonotrypaea harmandi* [see Tamaki and Kikuchi 1983, with the name, *Callianassa*  
70 *japonica*, incorrectly used (see Manning and Tamaki 1998; Yamada et al. 2017)]. Ghost shrimp are  
71 known for their bioturbation effects on sediment and consequent influences on benthic community  
72 structure and ecosystem functioning (Pillay and Branch 2011). In the present case, the *N. harmandi*

73 zone occupied the upper one-third part of the sandflat, with shrimp burrows extending over the  
74 whole, 10s-cm thick sediment column (above the mollusc shell layer). The accompanying sediment  
75 conditions, such as shifting surface sediment and fully oxidized sediment column, were ascribed to  
76 dense burrow stands and bioturbation of the shrimp (Tamaki 1984; Tamaki and Suzukawa 1991;  
77 Wardiatno et al. 2003). On an estuarine intertidal sandflat in South Africa, the density of a population  
78 of *U. grimaldii* in a bed of the ghost shrimp, *Callichirus kraussi*, changed in accordance with the  
79 experimental removal and subsequent recovery of the shrimp population (Wynberg and Branch  
80 1994). Populations of *U. grimaldii* occurred also on South African open sandy beaches with *C.*  
81 *kraussi* absent (Bally 1983). These observations suggest some commensalism of *Urothoe* spp. with  
82 ghost shrimp under sheltered settings. Either amphipod residence inside shrimp burrows or its  
83 attraction to bioturbated sediment to varying magnitude may be involved in the relationship.

84 One way narrowing down the above possibilities regarding the commensalism is to find  
85 amphipods embedded in transparent resin casts of ghost shrimp burrows. Another way is to examine  
86 temporal changes in the distributions of the amphipod and ghost shrimp. On the Tomioka sandflat,  
87 the sediment surface mixing over the whole shore is caused by seasonal wind-induced waves in the  
88 wintertime, while the surface outside the *N. harmandi* zone is stable in the summertime (Tamaki  
89 1984, 1987). After 1979, the distribution range of the *N. harmandi* population expanded, having  
90 occupied the entire sandflat by 1983 (Tamaki and Suzukawa 1991). This state has continued until  
91 2015 (Tamaki and Takeuchi 2016). Both seasonal change around 1979 and some later years'  
92 summertime distributions in the *U. carda* population would provide clues to clarifying its  
93 dependency on *N. harmandi*. In addition, the amphipod spatial distribution pattern might be different  
94 between sexes or between adults and juveniles relative to the ghost shrimp distribution. Finally, since  
95 *Urothoe* species are adapted to loosely packed sand (Bousfield 1970), the hardness of sediment may  
96 affect the distribution of *U. carda* in relation to that of *N. harmandi* on the present sandflat.

97 Undisturbed state of sediment hardness can be evaluated by vane shear strength *in situ*, where a thin  
98 vane blade is inserted into the sediment surface and the sediment maximum resistance to horizontal  
99 shearing associated with blade rotation measured (Amos et al. 1988; Sassa and Watabe 2007; Sassa  
100 et al. 2011, 2014). The sediment hardness assessed by vane shear strength has been shown to govern  
101 the burrowing performances of a crab (Sassa and Watabe 2008), bivalves (Sassa et al. 2011), and  
102 amphipods (Sassa et al. 2014) on intertidal sandflats and sandy beaches.

103 The objective of the present study was to show how the dependency of *U. carda* on *N. harmandi*  
104 is formed under a sheltered setting of the Tomioka sandflat and to what degree that commensalism  
105 is. First, relative to the ghost shrimp distribution and associated sediment conditions including depth  
106 of redox potential discontinuity layer and grain-size composition, the following items were  
107 examined for the amphipod population: zonation parallel to the shoreline in the summer of 1980;  
108 year-round change in the cross-shore distribution during 1980 to 1981; cross-shore distribution in  
109 four summers between 1984 and 2015; and cross-shore distributions of adults of both sexes and  
110 juveniles in 2015. Second, vertical distribution of amphipods in the sediment column and presence  
111 or absence of amphipods inside resin casts of shrimp burrows were checked. Finally, the cross-shore  
112 variation in sediment hardness was examined in relation to shrimp and amphipod distributions.

113

## 114 **Materials and methods**

### 115 **Monitoring density and distribution of macrofauna and substrate properties**

116 The Tomioka sandflat is located on the northwestern corner of Amakusa-Shimoshima Island  
117 (130.037°E; 32°521°N) situated west of Ariake Sound (largest estuary in Kyushu) under a semi-  
118 diurnal tidal regime (Fig. 1a). The maximum emerged area of the sandflat during low tide in spring-  
119 tide periods spans 3.5 km alongshore and 150–550 m cross-shore in Tomioka Bay, with the  
120 maximum tidal range of 3.3 m (Fig. 1b). A rectangular area for the census of macrofauna was

121 established around the northwestern corner of the sandflat, which was 300 m alongshore  $\times$  310–325  
122 m cross-shore [to the mean low water level in spring-tide periods (MLWS); Fig. 1c]. Although the  
123 census area is sheltered to some extent by the northwest- to north-lying headland and sand spit, yet  
124 landward transport of some surface-dwelling macrofauna is caused by northerly wind-induced waves  
125 during late autumn to early spring (Tamaki 1987; Tamaki and Takeuchi 2016). In the census area,  
126 four parallel, cross-shore transects were placed, which were named Transects A, E, G, and J, with the  
127 distance between adjacent transects being 60–120 m. On each transect, the stations for sampling  
128 were placed every 10 m from the uppermost one at either the sandflat landward edge or 10 m  
129 seaward of it to the lowest one at the MLWS; Stn X-Y designates Y m from the landward edge on  
130 Transect X. In the first census conducted in July 1979, four faunal assemblage zones quasi-parallel to  
131 the shoreline were delineated (Tamaki and Kikuchi 1983). Each zone was named after its dominant  
132 or characteristic species (or genus): from upper to lower shore, the spionid polychaete, *Prionospio*  
133 *aucklandica* (originally as *P. krusadensis*), *Nihonotrypaea harmandi* (originally as *Callianassa*  
134 *japonica*), the bivalve, *Solen strictus*, and the gastropod, *Umbonium moniliferum*. The cross-shore  
135 ranges were wider in the *Nihonotrypaea* and *Umbonium* zones than in the other two zones, nearly  
136 coincident with those of the habitats of *N. harmandi* and *U. moniliferum*. The whole sediment-  
137 column depth spanned 20–30 cm in the *Prionospio* and *Solen* zones, 30–40 cm in the *Nihonotrypaea*  
138 zone, and 50–60 cm in the *Umbonium* zone (Tamaki 1984; Takeuchi and Tamaki 2014).

139 Following the above first census' result, Transect G was selected as a representative transect to  
140 monitor the subsequent change in the zonation patterns of *Urothoe carda* and *N. harmandi*. The  
141 stations visited on each sampling occasion were selected as a subset from the above-mentioned  
142 maximum number of stations. The year-round monitoring was conducted during low tide in spring-  
143 tide periods from 18 March 1980 to 9 April 1981, most frequently every month. Eighteen to 22  
144 stations were visited on each sampling occasion. At each station, first, the thickness of redox

145 potential discontinuity (RPD) layer was measured for a sediment column extracted with a  
146 transparent acrylic tube of 100-cm<sup>2</sup> circular cross-sectional area × 35-cm length, in which that layer  
147 was identified as the position with clear color changes. Along the boundary circle, the thickness was  
148 measured to 1 mm on several points including troughs and crests of small ripples if present (up to  
149 1–1.5 cm in crest height) and the mean value calculated [data given in Tamaki (1984)] – briefly, (1)  
150 in the *Nihonotrypaea* zone, the entire sediment column was brown, suggesting an oxidized  
151 condition; (2) seaward of that zone by up to 40 m (mainly in the *Solen* zone), the surface brown layer  
152 was replaced by the gray layer at 10–20-cm depth; and (3) further seaward (in the *Umbonium* zone),  
153 the black-colored layer lay immediately below the brown layer at depths < 10 cm. In the present  
154 study, the brown layer bottom was defined as the RPD layer depth; in cases that it continued beyond  
155 25 cm, the RPD layer thickness was indicated uniformly as 25 cm in the Results. Second, the surface  
156 1-cm deep sediment was collected for granulometric analysis by the standard serial sieving protocol  
157 (Buchanan and Kain 1971). Three parameters [median  $\phi$  ( $Md\phi$ ), sorting coefficient ( $\sigma_1$ : inclusive  
158 graphic standard deviation), and mud content (percentage silt-clay fraction in weight)] were  
159 obtained. Third, the number of surface openings of *N. harmandi* burrows was counted for four  
160 adjacent 25- × 25-cm square plots haphazardly marked on the sandflat surface; one individual of *N.*  
161 *harmandi* dwells solitarily in its Y-shaped burrow with two openings (Tamaki and Ueno 1998). At  
162 any station in which all burrow-opening diameters were small (1–2-mm  $\phi$ ), as compared with a  
163 mixture of both small and large (3–6-mm  $\phi$ ) openings, such a station was recorded as that occupied  
164 by only new recruits of the year (Tamaki et al. 1997; Tamaki and Ueno 1998). Finally, at one of the  
165 four plots per station, a metal quadrat frame of the same size as above was inserted to a depth of 10  
166 cm and the sediment inside excavated, passed through a 0.5-mm mesh sieve, and fixed with 10%  
167 neutralized formalin solution for *U. carda* specimens. For the specimens collected in 2015, after  
168 their sexes were identified based on the number of articulation in flagellum of antenna 2, the mature

169 and immature categories were determined based on (1) ovigerous or non-ovigerous state (female),  
170 (2) presence or absence of calceoli in antenna 2 (male), and (3) total-length-frequency distributions  
171 (A. Tamaki et al., unpubl data) and the distributions of the four groups on Transect G examined.

172 On 10–11 August 1980, a census for the whole study area was made along the four transects  
173 (Fig. 1c; at 19–22 stations for each), following the same procedure as above.

174 After the complete expansion of the *N. harmandi* population over the sandflat in 1983 (Tamaki  
175 and Suzukawa 1991), sampling along Transect G was conducted in each late July–early August of  
176 1984, 1997, 2010, and 2015, basically following the same procedure as above, with some  
177 modifications. In 1997, 2010, and 2015, the sampling stations had to be altered according to the  
178 shortening of the transect length by 20 m due to the reclamation of the uppermost zone of the  
179 sandflat in 1991–1993 [see Tamaki and Takeuchi (2016) for details]. The most landward station was  
180 re-installed at the landward edge of the intact sandflat, which is named Stn G-0 (2010s). This station  
181 is identical to the previous Stn G-20, which is hereafter re-named Stn G-20 (1980s); note that the  
182 most landward station in the 1980s was Stn G-10, not Stn G-0. In cases for no misunderstanding  
183 about years, the parentheses with years are omitted. The position of the MLWS on the transect has  
184 been unchanged, which corresponds to Stn G-310 (1980s) and Stn G-290 (2010s). In 1984 and 1997,  
185 the surface burrow-opening count for *N. harmandi* was made at four adjacent unit ( $25 \times 25$ -cm<sup>2</sup>)  
186 plots, while in the 2010s, it was made at eight or nine plots. In 2015, at Stns G-10, 30, and 50, an  
187 acrylic tube with cross-sectional area of 100 cm<sup>2</sup> was used for collecting macrofauna, in which a  
188 combined sample of six 10-cm deep sediment columns was regarded as equivalent to the usual, one  
189 625-cm<sup>2</sup> quadrat sample. Granulometric analysis for the surface 1-cm sediment (3 cm only in 2015)  
190 was made by the standard serial sieving protocol for the samples until 1997 and by using a laser  
191 diffraction particle-size analyzer (SALD-3100, Shimazu) for those in the 2010s. To estimate the  
192 individual numbers of adults and newly-recruited juveniles of *N. harmandi* from the burrow-

193 opening-counts in 2015 from 16 stations (Stns G-0, -10, -30, and every 20-m increment to -290), 10  
194 samples of the whole sediment column were extracted with the coring tube at each of Stns G-30, -90,  
195 -150, -210, and -270, passed through a 0.5-mm mesh sieve, and fixed on 3 August 2016. In the  
196 laboratory, juveniles and adults were separated according to the distinct difference in body size.  
197 Based on a yearly stable tendency for the juvenile distribution pattern over the transect (Tamaki et al.  
198 1997), the juvenile-to-adult number ratio was applied to the 2015 data, in which the two adjacent  
199 stations about each of the above five stations with core samples were assumed to take the same ratio  
200 (the ratio at Stn G-30 was applied also to Stn G-0).

201 During  $\pm 1$  h around the lowest-tide time on 1 August 2015, the surface elevation along Transect  
202 G was measured to 1 mm with TRIMBLE R4 GNSS System (Trimble). At each of Stns G-0 to -290  
203 (16 stns), the level of the groundwater table was measured to 1 mm with a ruler 1 min after  
204 shoveling the surface sediment. Then, sediment hardness for the sub-surface depths of 10 mm and 40  
205 mm were measured with a vane blade of 40-mm  $\phi$  and 10-mm depth (FTD2CN-S, Seiken) and of  
206 20-mm  $\phi$  and 40-mm depth (FTD5CN-S, Seiken), respectively, at a point randomly placed between  
207 surface burrow openings of *N. harmandi*. To compare the sediment hardness values at 10-mm depth  
208 among the sediments containing a small burrow opening with 1–2-mm  $\phi$ , a large one with 4–6-mm  
209  $\phi$ , and outside burrow openings, measurements were made with FTD2CN-S at a location with high  
210 shrimp densities around the lowest-tide time on 1 August 2016 ( $n = 6$  for each burrow-opening size  
211 and  $n = 13$  for the latter). In the measurement for the former two, the center of the vane blade was  
212 positioned exactly at each burrow opening. In both 2015 and 2016, the weather was fine and calm.

213

#### 214 **Vertical distribution of *U. carda* in the sediment column**

215 To determine the vertical distribution of *U. carda* individuals in the substrate inhabited by *N.*  
216 *harmandi* on the Tomioka sandflat during low tide, sediment columns were extracted with a

217 graduated acrylic tube, and sectioned into multiple layers, passed through a 0.5-mm mesh sieve, and  
218 fixed with 10% neutralized formalin solution. On 15 August 1981, each of the three sediment  
219 columns of a cross-sectional area of 100 cm<sup>2</sup> to a 23-cm depth (brown in color) at Stn G-20 were  
220 sectioned into six layers of 0 (= surface)–1, 1–2, 2–3, 3–5, 5–10, and 10–23 cm and the samples for  
221 each layer combined. On 13 May 2017, each of the six sediment columns of a cross-sectional area of  
222 24 cm<sup>2</sup> to a 15-cm depth (brown in color) at Stn G-30 were sectioned into three layers of 0–5, 5–10,  
223 and 10–15 cm and the samples for each layer combined.

224

#### 225 **Casting burrows of *N. harmandi***

226 To examine whether or not individuals of *U. carda* dwell inside *N. harmandi* burrows, polyester  
227 resin casts of aggregated burrows were made over a circular area enclosed with a 23.5-cm  $\phi$  bottom-  
228 removed polypropylene container around Stn G-10 on the Tomioka sandflat during low tides from  
229 27 to 28 May 2017, following the burrow casting protocol given in Tamaki and Ueno (1998). In the  
230 laboratory, amphipods embedded in the transparent burrow casts were searched for.

231

#### 232 **Results**

##### 233 **Vertical distribution of *Urothoe carda* in the sediment column**

234 In August 1981, all 191 individuals of *Urothoe carda* in the 23-cm deep sediment column on the  
235 Tomioka sandflat were found from the upper 5-cm layer, with 14% in 0–1 cm, 56.5% in 1–2 cm,  
236 23.5% in 2–3 cm, and 6% in 3–5 cm. In May 2017, 112 of a total of 113 individuals present in the  
237 15-cm deep sediment column were found from the upper 5-cm layer, with 1 individual in 5–10 cm.

238

##### 239 **Burrow casts of *Nihonotrypaea harmandi***

240 In the 434-cm<sup>2</sup> enclosed area of the Tomioka sandflat in May 2017, the number of casts of Y-

241 shaped burrows of *Nihonotrypaea harmandi* was 34, including those with either one of the two  
242 segments above the node of the *Y* incomplete (Fig. 2). The maximum depth of each burrow ranged  
243 from 9.0 to 27.1 cm, with mean ( $\pm$  SD) being 18.2 ( $\pm$  5.8) cm. The depth of the node of the *Y* ranged  
244 from 6.7 to 16.9 cm, with mean ( $\pm$  SD) being 11.6 ( $\pm$  2.4) cm. The number of casts with only a  
245 single shaft retrieved was 19. No individuals of *U. carda* were embedded in the burrow casts, with  
246 341 expected individuals residing in the surface 5-cm layer of the enclosed area, based on their  
247 nearby density (113 inds 144 cm<sup>-2</sup>; preceding sub-section).

248

#### 249 **Temporal change in the transect distributions of *N. harmandi* and *U. carda* during 1980–1981**

250 Over the four transects on the Tomioka sandflat on 10–11 August 1980, *N. harmandi* burrows  
251 and *U. carda* individuals showed a common zonation pattern quasi-parallel to the shoreline (Fig. 3).  
252 The main zone occupied by *N. harmandi* burrows, with RPD depths  $\geq$  25 cm, shifted from the upper  
253 half of Transect J to the upper one-third of Transect A. The overall mean ( $\pm$  SD) *N. harmandi* density  
254 from mean density at every station with a non-zero value (including the stations with RPD depths <  
255 25 cm), as estimated from burrow-opening counts, was 182 ( $\pm$  138) shrimps m<sup>-2</sup> [ $n$  = 35 (stns)].  
256 Almost all individuals of *U. carda* occurred in the main *N. harmandi* zone, with mean density over  
257 the four transects being 43.8 inds 625 cm<sup>-2</sup> ( $n$  = 77). On each transect, two separate density-peaks  
258 were present in the upper and mid- to lower part of the *Nihonotrypaea* zone, respectively. On  
259 Transects G, E, and A, a substantial part of each transect population of *U. carda* occurred also 10–20  
260 m seaward of the seaward limit of the *N. harmandi* zone (i.e. in the *Solen* zone), with RPD depths of  
261 10–17 cm. Beyond the *Solen* zone [i.e. in the *Umbonium* zone (to the MLWS)], the RPD depths lay  
262 closer to the surface, with mean ( $\pm$  SD) for the four transects being 3.4 ( $\pm$  1.2) cm ( $n$  = 30).

263 Along Transect G during March 1980 to April 1981, the seaward limit of the *N. harmandi* adult-  
264 inhabited zone expanded by 20 m, from Stn G-130 to Stn G-150, in October, when Stn G-260 was

265 also established as a separate zone in the lower shore (gray columns in Fig. 4a–m). This colonization  
266 was caused by both adult immigration and settlement of new recruits (Tamaki and Ingole 1993;  
267 Tamaki 1994). The overall mean density through the year estimated from the mean burrow-opening  
268 density at every station with a non-zero value was 181 shrimps  $m^{-2}$  ( $n = 170$ ). The mean density of  
269 *U. carda* on each sampling occasion ranged from 57.9 (May 1980) to 102.0 (April 1980) inds 625  
270  $cm^{-2}$ , with overall mean ( $\pm$  SD) through the year being 81.7 ( $\pm$  13.1) inds 625  $cm^{-2}$  ( $n = 13$ ). The  
271 population of *U. carda* showed a clear seasonal distribution pattern relative to the *Nihonotrypaea*  
272 zone. During July to September, most of the population was confined to the *Nihonotrypaea* zone,  
273 and a substantial part was extended beyond that zone to the lowest shore during December to May,  
274 with the distributions in June and October transitional. The extended and contracted phases of the *U.*  
275 *carda* population in the *Umbonium* zone (Stns G-180–310) were in parallel with the seasonally  
276 changing RPD depths, of which mean ( $\pm$  SD) values were 6.8 ( $\pm$  2.4) cm ( $n = 21$ ) during March to  
277 May 1980, 5.0 ( $\pm$  2.7) cm ( $n = 7$ ) in June, 2.6 ( $\pm$  1.0) cm ( $n = 38$ ) during July to September, 5.1 ( $\pm$   
278 2.1) cm ( $n = 6$ ; excluding Stn G-260) in October, and 6.2 ( $\pm$  1.5) cm ( $n = 18$ ; excluding Stn G-260)  
279 during December 1980 to April 1981. During June to October, there were largely two separate  
280 density-peaks of *U. carda* in the upper and mid- to lower *Nihonotrypaea* zone, respectively, and a  
281 substantial part of the transect population occurred 10–30 m seaward of the seaward limit of the *N.*  
282 *harmandi* adult-inhabited zone (i.e. in the *Solen* zone), with RPD depths of 8–16 cm. At Stn G-260  
283 in October, both *N. harmandi* density (mean of 240 shrimps  $m^{-2}$ ) and RPD depth (12 cm) were  
284 greater than those values at the other lower-shore stations. The *U. carda* density was higher at Stn G-  
285 260 than at the two adjacent stations.

286

### 287 **Temporal change in the transect distributions of *N. harmandi* and *U. carda* during 1984–2015**

288 Along Transect G on the Tomioka sandflat in 1984, 1997, 2010, and 2015, all stations were

289 occupied by *N. harmandi*, with mean ( $\pm$ SD) shrimp densities over the stations (inds  $m^{-2}$ ), as  
290 estimated from burrow-opening counts, declining from 461 ( $\pm$  104) in 1984 [ $n$  = 16 (stns); Stn G-10  
291 (uppermost station: *Prionospio* zone) excluded], via 214 ( $\pm$  63) in 1997 ( $n$  = 15; Stn G-0 excluded),  
292 to 69 ( $\pm$  38) in 2010 ( $n$  = 18) and 104 ( $\pm$  38) in 2015 ( $n$  = 16) (Fig. 5a–d). The marked reduction in  
293 shrimp densities from 1984 to 1997 was caused by heavy predation by the stingray, *Dasyatis akajei*,  
294 which continued from 1995 onward (up to the present) (Takeuchi and Tamaki 2014; Tamaki and  
295 Takeuchi 2016). Stingrays excavate deep pits during foraging for shrimps, which had the maximum  
296 impact on the shrimp population in the mid-shore due to the thinnest sediment columns there (20s  
297 cm; Takeuchi and Tamaki 2014). Also in 2010, the spatially different stingray impact was reflected  
298 in the higher shrimp densities in the upper and lower shores and the lowest ones in the mid-shore. In  
299 2015, the densities in the mid-shore were not lower than in the upper and lower shores. This was  
300 most probably due to the higher new recruits' densities in the mid- to lower shore, as indicated in the  
301 distribution of estimated densities of juveniles and adults over the transect (Fig. 5e).

302 In 1984, 1997, and 2015, the RPD depths were > 25 cm at all stations except for Stn G-10 (data  
303 not shown in Fig. 5). In 2010, although most RPD depths were > 25 cm, the values of 8–20 cm  
304 emerged in the mid-shore (Fig. 5c).

305 In 1984, *Urothoe carda* occurred over the whole transect, with 26–147 (range) and 74.2 [mean;  $n$   
306 = 17 (stns)] inds  $625\text{ cm}^{-2}$  (Fig. 5a; hereafter  $625\text{ cm}^{-2}$  is omitted for density values). In 1997, the  
307 densities over the whole transect were lower than in 1984, with up to 65 inds and the mean of 9.3  
308 inds ( $n$  = 16), and 75% of the whole members occurred from the upper 50-m part of the transect  
309 (Fig. 5b). In 2010, the same tendency as in the ghost shrimp distribution was observed, with the  
310 highest *U. carda* densities of 51 and 105 inds being at Stns G-30 and G-220, respectively, and the  
311 mean density over the whole transect being 34.6 inds ( $n$  = 18) (Fig. 5c). Also in 2015, the lower  
312 densities in the mid-shore was sandwiched by the highest densities in the upper and lower shores

313 (107–108 and 125 inds at Stns G-30–G-50 and G-270, respectively), with the mean density over the  
314 whole transect being 64.4 inds ( $n = 16$ ) (Fig. 5d). The spatial variation in the density of *U. carda*  
315 resembled that of *N. harmandi* adults (Fig. 5e). Furthermore for *U. carda*, in the upper-half shore,  
316 the mature and immature individuals of both sexes were distributed separately in its lower and upper  
317 parts, while in the lower-half shore, the distribution centers of mature and immature individuals of  
318 both sexes were at the two lowest stations, decreasing toward each lowest density at Stn G-130,  
319 though the tendency in the mature male was less clear due to its low densities (Fig. 5f).

320

### 321 **Temporal change in sediment grain-size composition and snapshot underground properties**

322 The distributions of  $Md\phi$ ,  $\sigma_1$ , and mud content of the surface sediment along Transect G on the  
323 Tomioka sandflat in July–August of 1980–2015 are shown in Fig. 6a–c, respectively. In all years,  
324 the particle was finer landward, as is general for tidal flats. In 1980 and 1984, from lowest to  
325 uppermost shores, the sediment type shifted from well-sorted to moderately-sorted, fine to coarser  
326 very fine sand. The mud content in 1980 exhibited a dip in the lower part of the *Nihonotrypaea* zone  
327 (Stns G-20–G-130). In 1997, as compared with the 1980s, especially in the transect mid- to lowest  
328 part, (1) median particle diameter became slightly larger within the fine sand category, (2) sorting  
329 became largely better within the moderately well-sorted category, and (3) mud content became less.  
330 This trend continued afterward, especially with a marked increase in median grain size and decrease  
331 in mud content. In 2010 and 2015, from lowest to uppermost shore, basically, the values of  $Md\phi$   
332 shifted from medium to coarser-fine sand categories, and the values of  $\sigma_1$  shifted from very well- to  
333 moderately-sorted categories. The greater spatial variations in the  $Md\phi$  and  $\sigma_1$  in 2015 than in 2010  
334 might be due to the deeper sediment samples in the former with greater heterogeneities (3 vs. 1 cm).  
335 The locally high mud contents at Stns G-150 and -190 in 2010 corresponded to the lowest densities  
336 of *N. harmandi* there (Fig. 5c).

337 The sandflat surface elevation inclined gently along Transect G in 2015, with a gradient of ca.  
338 1/250 over 290 m. The groundwater tables were close to the sandflat surface [range = -2.5 (below  
339 surface) to 2.5 (above surface: overflow) cm; mean ( $\pm$  SD) = 0.6 ( $\pm$  1.4) cm;  $n$  = 16 (stns)]. The  
340 distribution of sediment hardness over the transect is shown in Fig. 7. The vane shear strengths at 4-  
341 cm depth were higher in the upper and lower shores and lowest in the mid-shore, coincident with the  
342 spatial variation in the densities of both *U. carda* individuals (Fig. 5d, f) and *N. harmandi* adults  
343 (Fig. 5e), while those strengths at 1-cm depth varied in a small range around a much lower value.

344 In comparing the values of sediment hardness among the points at small and large burrow  
345 openings of *N. harmandi*, and at outside-burrow-opening points in 2016, the value for sediments on  
346 another intertidal sandflat [Okoshiki sandflat in Ariake Sound (cf. Yamada and Kobayashi 2007);  
347 Fig. 1a] during low tide in 2010 were used additionally ( $n$  = 5; S. Sassa and S. Yang, unpubl data)  
348 (Fig. 8). That sandflat is dominated by large sand waves and shares essentially the same sediment  
349 granulometric characteristics (median diameters: 0.18–0.28 mm) and the groundwater table up to the  
350 surface (in troughs of the sand waves) with those of the Tomioka sandflat. Although a large number  
351 of *N. harmandi* and *N. japonica* existed in 1998 (Wardiatno et al. 2003), no surface burrow openings  
352 of both species were found at the time of measurement in 2010 (points with “no burrow openings”).  
353 The lowered abundance of *N. japonica* population in recent years are common to several intertidal  
354 sandflats in Ariake Sound (Takeuchi et al. 2013). The difference in the median values of vane shear  
355 strength among the four points was tested for significance by Kruskal-Wallis test, followed by Steel-  
356 Dwass multiple comparison test, using “R”-based software “EZR” (Kanda 2013). There was a  
357 significant difference among the four points (Kruskal-Wallis  $\chi^2 = 25.7$ ,  $df = 3$ ,  $P < 0.001$ ), and the  
358 mean-value order from high to low was: large burrow opening, small burrow opening, no burrow  
359 openings, and outside-burrow openings. Except for the pair between small and no burrow openings,  
360 all other pairs were significantly different ( $P < 0.01$  or 0.05).

361

362 **Discussion**

363 The stable association of *Urothoe carda* with *Nihonotrypaea harmandi* on the Tomioka sandflat  
364 was evident from (1) their common upper-shore distribution on the four transects in the summer of  
365 1980 (Fig. 3) and on one of these transects (Transect G) in the summertime of 1980 (Fig. 4e–i) and  
366 (2) their whole-shore distributions on Transect G in the summers of 1984, 2010, and 2015, when the  
367 entire sandflat had been occupied by *N. harmandi* (Fig. 5a, c, d). Through these years, the mean  
368 density of *U. carda* (no. inds 625 cm<sup>-2</sup>) over Transect G varied in a small range from 35 to 82. The  
369 mean density value was 9 in 1997, when most individuals were in the upper part of the transect  
370 despite the whole-shore distribution of *N. harmandi* (Fig. 5b). It is thus inferred that the base of the  
371 *U. carda* population lay primarily in the upper *N. harmandi* zone and that, in its higher-abundance  
372 phase, *excess* individuals of the *U. carda* population made a range extension into the mid- to lower  
373 *N. harmandi* zone. Frequent shuffling their dwelling sites on the present sandflat during nocturnal  
374 submergence periods is suggested (A. Tamaki et al., unpubl data). In 2010 and 2015, the *U. carda*  
375 densities peaked in the upper and lower shores separately, with the lowest densities in the mid-shore  
376 (Fig. 5c, d). This was in parallel with the spatial variation in the *N. harmandi* density, especially that  
377 of adults, not of juveniles (Fig. 5e, f). In the upper-half shore in 2015, the center of the distributions  
378 of mature individuals (adults) of both sexes of *U. carda* was at 90 m from the uppermost shoreline,  
379 while that of immature individuals (juveniles) was within 50 m from there (Fig. 5f). Such a bimodal  
380 distribution within the upper shore was observed on most sampling occasions during 1980 to 1981  
381 (Figs. 3 and 4), which might have also been due to the segregation of adults and juveniles. The peak  
382 position of juveniles situated landward of that of adults was recorded for a number of macrobenthic  
383 species on the present sandflat, which was suggested to be caused by hydrodynamic sorting by body  
384 size (Tamaki 1987; Tamaki and Suzukawa 1997; Tamaki and Takeuchi 2016). The salinity of the

385 groundwater along Transect G measured during low tide in June, 1998 indicated the values of  
386 9.0–17.4 in the upper 50-m zone and 31.2–32.0 in the seaward zone, suggesting the penetration of  
387 ground freshwater from the land into the former zone (Wardiatno et al. 2003). The low salinity in the  
388 upper sandflat may be sub-optimum for *U. carda* adults but optimum for some species including  
389 *Prionospio aucklandica* and the anthurid isopod, *Cyathura muromiensis* (see Tamaki and Kikuchi  
390 1983). On some intertidal sandflats, a peculiar benthic assemblage occurred in each uppermost area  
391 with ground freshwater discharge (Zipperle and Reise 2005; Dale and Miller 2008).

392 Despite its long-term stability, the association between *U. carda* and *N. harmandi* on the  
393 Tomioka sandflat was not always obligate. This was evident from the observations on the extended  
394 distribution of *U. carda* beyond the *N. harmandi*-inhabited zone by 10–30 m seaward along the four  
395 transects and Transect G in the summer of 1980 (Figs. 3 and 4d–g) and by all remaining length of  
396 Transect G during winter to spring in 1980 and 1981 (Fig. 4a–c, k–m). Thus, *U. carda* can be  
397 regarded as a facultative commensal of *N. harmandi*. As no individuals of *U. carda* were found  
398 inside the resin casts of *N. harmandi* burrows (Fig. 2), they are assumed to exist in the interstitial  
399 space between these burrows. Such a micro-scale distribution pattern is similar to that of *U.*  
400 *poseidonis* associated with, but not inside, the tubes of the terebellid polychaete, *Lanice conchilega*,  
401 on an intertidal sandflat (Callaway 2006). The dwelling depth in the sediment column was 0–5 cm  
402 for *U. carda* and down to 10–15 cm for *U. poseidonis* (see Lackschewitz and Reise 1998; Callaway  
403 2006). A similar association between free-burrowing amphipod and ghost shrimp may exist for *U.*  
404 *grimaldii* and *Callichirus kraussi* on South African estuarine intertidal sandflats (cf. Wynberg and  
405 Branch 1994). Facultative commensalism of smaller macrobenthos with *N. harmandi* on the present  
406 sandflat was reported for the cirrolanid isopod, *Eurydice nipponica*, which primarily occurs on  
407 exposed sandy beaches along the coastline of Kyushu (Tamaki and Suzukawa 1991, 1997). Some  
408 bioturbation effects of *N. harmandi* would become beneficial to both *U. carda* and *E. nipponica*

409 under the present sheltered setting. Compared with *U. carda*, *E. nipponica* was confined to the  
410 *Nihonotrypaea* zone year-round in 1980–1981, and not only distribution range but also population  
411 size increased from 1984 onward (Tamaki and Suzukawa 1991, 1997; A. Tamaki, unpubl data).  
412 Though either facultative or obligate one is unknown, callianassids-associated commensalism in  
413 highly mobile smaller macrobenthos on sandy bottoms was reported for ostracods (Riddle 1988),  
414 amphipods (Posey 1986; Riddle 1988), bivalves (Aller and Dodge 1974; Tudhope and Scoffin 1984),  
415 and polychaetes (Riddle 1988; Wynberg and Branch 1994).

416 For *U. poseidonis* individuals associated with their presumed polychaete hosts, the sub-surface  
417 permeable sediment around those burrows or tubes was suggested to form an attractive interstitial  
418 space with elevated dissolved oxygen concentration and/or increased food supply (Lackschewitz and  
419 Reise 1998; Callaway 2006). Increased permeability in the sediment may also enable the amphipod  
420 to filter-feed more efficiently there (cf. Bousfield 1970). The thickness of the surface oxidized layer  
421 in yellow or brown color above the RPD depth, with the reduced layer beneath it in gray to black  
422 colors, nearly coincides with the thickness of the surface oxygenated layer on sheltered intertidal  
423 sandflats and dissipative sandy beaches (Fenchel and Riedl 1970; McLachlan 1978; McLachlan and  
424 Turner 1994). Thus, although pore-water dissolved oxygen concentration of the sediment was not  
425 measured in the present study, the surface oxidized sediment layer thickness (SOSLT) could be used  
426 as a proxy for the surface oxygenated sediment layer thickness. Consistently through 1980 to 2015,  
427 the whole sediment column in the zone densely inhabited by *N. harmandi* adults was oxidized,  
428 where the population of *U. carda* mainly occurred (Figs. 3–5). The oxidized substrate also affects  
429 the bacterial community on the present sandflat (Wada et al. 2016). The surface sediment's greater  
430 median size, better sorting, and lower content of silt-clay that took place through these years (Fig.  
431 6a–c) could also make the sediment more permeable. These granulometric parameter changes might  
432 have been caused by the bioturbation of *N. harmandi*, horizontally expelling finer fractions of the

433 surface sediment away and burying its very coarser fraction deep into the sediment column (Tamaki  
434 1994; Wardiatno et al. 2003), of which mechanism remains to be examined. The range of those  
435 sediment grain-size parameter values through all years appears acceptable by *U. carda*. In the zone  
436 seaward of the *N. harmandi*-inhabited upper shore during 1980 to 1981, the SOSLT and the  
437 intermediate to high densities of *U. carda* occurred coincidentally: (1) the extended distributions of  
438 both oxidized sediment column and *U. carda* by 10–30 m seaward (into the *Solen* zone) in the  
439 summertime, (2) the smallest SOSLT and the absence or quite low densities of *U. carda* beyond the  
440 *Solen* zone in the summertime, with dense spionid polychaete tube mats in the *Solen* to upper  
441 *Umbonium* zone (Tamaki and Kikuchi 1983; Tamaki 1984, 1985), and (3) the larger SOSLT and the  
442 intermediate or high densities of *U. carda* in the *Solen* to *Umbonium* zones through the winter and  
443 early spring. The threshold SOSLT allowing the existence of *U. carda* appeared to be 5 cm (Figs. 3  
444 and 4), which was equal to the maximum depth of *U. carda* individuals in the sediment column.  
445 Regarding a possible mechanism causing the above event (1), it is noteworthy that the hydraulic  
446 activity of the ghost shrimp, *Neotrypaea californiensis*, induced lateral transport of oxygenated water  
447 into the surrounding sediment as well as into their burrows in laboratory aquaria (Volkenborn et al.  
448 2012). Woodin et al. (2010) proposed that those large bioturbators residing in burrows with  
449 permeable walls, including arenicolid polychaetes, be called infaunal hydraulic ecosystem engineers.  
450 The seasonal change in the SOSLT in the above events (2) and (3) was in accordance with that of the  
451 sediment silt-clay content at Stn G-160 (1980s), ranging from 0.7% in winter to 1.7% in summer,  
452 and with the greater degree of the sediment surface mixing by northerly wind-induced waves during  
453 the late autumn to early spring (Tamaki 1984, 1987). Such a seasonal change is generally found for  
454 sheltered intertidal sandflats, with the deposition of oxygen-consuming organic matter during the  
455 warmer and calmer season and the wind-wave disturbance during the colder and stormier season  
456 (Fenchel and Riedl 1970; McLachlan 1978).

457 The lateral and vertical sediment displacement by the *N. harmandi* population in high densities  
458 on the Tomioka sandflat may soften its inter-burrow substrate for *U. carda* individuals to efficiently  
459 move through and re-burrow into. The sediment hardness of intertidal sandflats depends on suction  
460 (i.e. negative pore water pressure relative to atmospheric pressure) and their packing states, the latter  
461 changing considerably with suction dynamics under tide-induced groundwater table fluctuations  
462 (Sassa and Watabe 2007). On sandy beaches, the sediment hardness due to suction development and  
463 suction-dynamics-induced sediment compaction acted as a limiting factor for the survival and  
464 distributions of amphipods (*Talorchestia brito* and *Haustorioides japonicus*) by preventing their  
465 burrowing behavior (Sassa et al. 2014). On the Tomioka sandflat, the groundwater table was nearly  
466 the same as the surface elevation during low tides, indicating that suction is absent throughout tidal  
467 cycles and that the hardness of the sediment depends solely on its packing state. The shape of the  
468 outline of vane shear strengths at 4-cm depth over Transect G (Fig. 7) was very similar to that for  
469 adult *N. harmandi* density (Fig. 5e) [and for *U. carda* density (Fig. 5f)]. This would have reflected a  
470 work for rotating the vane blade to destroy burrows encountered at that depth (Fig. 2), which was  
471 confirmed by the highest shear strength value at 1-cm depth exactly beneath the large burrow  
472 openings and the second highest value exactly beneath the small burrow openings recorded in 2016  
473 (Fig. 8). The 1-cm depth shear strengths in 2015 comparable to those outside and lower than at  
474 burrows in 2016 would represent the packing state of the sediment outside *N. harmandi* burrows.  
475 Such outside-burrow-opening shear strength on the Tomioka sandflat was significantly lower than  
476 the shear strength with no burrows on the Okoshiki sandflat (Fig. 8), despite the same sediment-Mdp  
477 ranges between the two sandflats and no suctions during low tides in trough parts of sand waves on  
478 the latter sandflat (Yamada and Kobayashi 2007; Sassa and Watabe 2009). This suggests that the  
479 bioturbating activity of *N. harmandi* individuals altered the sediment packing state through the  
480 displacement and rearrangement of sand particles among their highly dense burrows, which resulted

481 in the looser and more permeable sediments than those solely subjected to physical displacement.

482 In conclusion, for some species of *Urothoe* on sheltered intertidal sandflats, the bioturbation or  
483 tube/burrow of some large macrobenthos would provide amphipods with more permeable and softer  
484 sediments, generating elevated dissolved oxygen concentration and increased pore space to possibly  
485 facilitate amphipods' efficient burrowing and filter-feeding. Facultative commensalism of highly  
486 mobile species with those sedentary large macrofauna would form one stable functional component  
487 of the benthic community among other components on sheltered sandflats, including the one due to  
488 amensalism exerted from ghost shrimps on filter-feeding molluscs (e.g. Tamaki and Takeuchi 2016).

489

#### 490 **Acknowledgements**

491 We thank K. Hayashi, T. Hasegawa, S. Miyabe, H. Ueno, H. Kimura, Y. Tanaka, C. Matsumoto,  
492 Y. Sato, T. Nakagawa, and K. Watanabe for help in the field work. The water-depth data were  
493 provided by Hydrographic and Oceanographic Department, Japan Coast Guard. We appreciate  
494 constructive comments from the three reviewers.

495

#### 496 **Compliance with ethical standards**

497 **Funding** This study was partly supported by the Japan Society for the Promotion of Science  
498 Grants-in-Aid for Scientific Research JP26440244 to AT and JP15H02265 to SS.

499

500 **Conflict of interest** The authors declare that they have no conflict of interest.

501

502 **Ethical approval** All applicable international, national, and/or institutional guidelines for the  
503 care and use of animals were followed.

504

505 **References**

- 506 Aller RC, Dodge RE (1974) Animal–sediment relations in a tropical lagoon Discovery Bay, Jamaica.  
507 J Mar Res 32:209–232
- 508 Amos CL, Van Wagoner NA, Daborn GR (1988) The influence of subaerial exposure on the bulk  
509 properties of fine-grained intertidal sediment from Minas Basin, Bay of Fundy. Estuar Coast  
510 Shelf Sci 27(1):1–13. doi: 10.1016/0272-7714(88)90028-5
- 511 Bally R (1983) Intertidal zonation on sandy beaches of the west coast of South Africa. Cahiers de  
512 Biologie Marine 24:85–103
- 513 Barnard JL, Karaman GS (1991) The families and genera of marine gammaridean Amphipoda  
514 (except marine Gammaroidea). Part 2. Records of the Australian Museum Supplement  
515 13(2):419–866. doi: 10.3853/j.0812-7387.13.1991.367
- 516 Bousfield EL (1970) Adaptive radiation in sand-burrowing amphipod crustaceans. Chesapeake Sci  
517 11(3):143–154. doi: 10.2307/1351237
- 518 Buchanan JB, Kain JM (1971) Measurement of the physical and chemical environments. In: Holme  
519 NA, McIntyre AD (eds) Methods for the Study of Marine Benthos. Blackwell, Oxford, pp 30–58
- 520 Callaway R (2006) Tube worms promote community change. Mar Ecol Prog Ser 308:49–60. doi:  
521 10.3354/meps308049
- 522 Dale RK, Miller DC (2008) Hydrologic interactions of infaunal polychaetes and intertidal  
523 groundwater discharge. Mar Ecol Prog Ser 363:205–215. doi: 10.3354/meps07455
- 524 Fenchel TM, Riedl RJ (1970) The sulfide system: a new biotic community underneath the oxidized  
525 layer of marine sand bottoms. Mar Biol 7(3):255–268. doi: 10.1007/BF00367496
- 526 Fernandez-Gonzalez V, Fernandez-Jover D, Toledo-Guedes K, Valero-Rodriguez JM, Sanchez-Jerez  
527 P (2014) Nocturnal planktonic assemblages of amphipods vary due to the presence of coastal  
528 aquaculture cages. Mar Environ Res 101:22–28. doi: 10.1016/j.marenvres.2014.08.001

529 Fincham AA (1970) Amphipods in the surf plankton. *J Mar Biol Assoc UK* 50(1):177–198. doi:  
530 10.1017/S0025315400000709

531 Kanda Y (2013) Investigation of the freely available easy-to-use software ‘EZR’ for medical  
532 statistics. *Bone Marrow Transplant* 48:452–458. doi: 10.1038/bmt.2012.244

533 Lackschewitz D, Reise K (1998) Macrofauna on flood delta shoals in the Wadden Sea with an  
534 underground association between the lugworm *Arenicola marina* and the amphipod *Urothoe*  
535 *poseidonis*. *Helgoländer Meeresunters* 52(2):147–158. doi: 10.1007/BF02908744

536 Manning RB, Tamaki A (1998) A new genus of ghost shrimp from Japan (Crustacea: Decapoda:  
537 Callianassidae). *Proc Biol Soc Wash* 111(4):889–892

538 McLachlan A (1978) A quantitative analysis of the meiofauna and the chemistry of the redox  
539 potential discontinuity zone in a sheltered sandy beach. *Estuar Coast Shelf Sci* 7(3):275–290. doi:  
540 10.1016/0302-3524(78)90110-X

541 McLachlan A, Turner I (1994) The interstitial environment of sandy beaches. *PSZN I: Mar Ecol*  
542 15(3–4):177–211. doi: 10.1111/j.1439-0485.1994.tb00053.x

543 Pillay D, Branch GM (2011) Bioengineering effects of burrowing thalassinidean shrimps on marine  
544 soft-bottom ecosystems. *Oceanogr Mar Biol Annu Rev* 49:137–192

545 Posey MH (1986) Changes in a benthic community associated with dense beds of a burrowing  
546 deposit feeder, *Callianassa californiensis*. *Mar Ecol Prog Ser* 31:15–22

547 R Core Team (2015) R: a language and environment for statistical computing. R Foundation for  
548 Statistical Computing, Vienna, Austria. URL <https://www.R-project.org/>. Accessed 11 Oct 2017

549 Riddle MJ (1988) Cyclone and bioturbation effects on sediments from coral reef lagoons. *Estuar*  
550 *Coast Shelf Sci* 27:687–695. doi: 10.1016/0272-7714(88)90075-3

551 Sassa S, Watabe Y (2007) Role of suction dynamics in evolution of intertidal sandy flats: field  
552 evidence, experiments, and theoretical model. *J Geophys Res* 112:F01003. doi:

553 10.1029/2006JF000575

554 Sassa S, Watabe Y (2008) Threshold, optimum and critical geoenvironmental conditions for  
555 burrowing activity of sand bubbler crab, *Scopimera globosa*. Mar Ecol Prog Ser 354:191–199.  
556 doi: 10.3354/meps07236

557 Sassa S, Watabe Y (2009) Persistent sand bars explained by geodynamic effects. Geophys Res Lett  
558 36:L01404. doi:10.1029/2008GL036230

559 Sassa S, Watabe Y, Yang S, Kuwae T (2011) Burrowing criteria and burrowing mode adjustment in  
560 bivalves to varying geoenvironmental conditions in intertidal flats and beaches. PLoS ONE  
561 6(9):e25041. doi: 10.1371/journal.pone.0025041

562 Sassa S, Yang S, Watabe Y, Kajihara N, Takada Y (2014) Role of suction in sandy beach habitats and  
563 the distributions of three amphipod and isopod species. J Sea Res 85:336–342. doi:  
564 10.1016/j.seares.2013.06.005

565 Sudo H (1988) Diurnal rhythms in predatory fish and amphipod prey. In: Hanyu I, Tabata M (eds)  
566 Daily Rhythmic Activities in Aquatic Animals. Kouseisha-Kouseikaku, Tokyo, pp 117–183 (in  
567 Japanese)

568 Takeuchi S, Tamaki A (2014) Assessment of benthic disturbance associated with stingray foraging  
569 for ghost shrimp by aerial survey over an intertidal sandflat. Cont Shelf Res 84:139–157. doi:  
570 10.1016/j.csr.2014.05.007

571 Takeuchi S, Takahara Y, Agata Y, Nasuda J, Yamada F, Tamaki A (2013) Response of suspension-  
572 feeding clams to natural removal of bioturbating shrimp on a large estuarine intertidal sandflat in  
573 western Kyushu, Japan. J Exp Mar Biol Ecol 448:308–320. doi: 10.1016/j.jembe.2013.07.018

574 Tamaki A (1984) Structural characteristics of an intertidal sand flat in Tomioka Bay, Amakusa, west  
575 Kyushu. Publ Amakusa Mar Biol Lab Kyushu Univ 7:125–150

576 Tamaki A (1985) Inhibition of larval recruitment of *Armandia* sp. (Polychaeta: Opheliidae) by

577 established adults of *Pseudopolydora paucibranchiata* (Okuda) (Polychaeta: Spionidae) on an  
578 intertidal sand flat. J Exp Mar Biol Ecol 87(1):67–82. doi: 10.1016/0022-0981(85)90193-5

579 Tamaki A (1987) Comparison of resistivity to transport by wave action in several polychaete species  
580 on an intertidal sand flat. Mar Ecol Prog Ser 37:181–189

581 Tamaki A (1994) Extinction of the trochid gastropod, *Umboonium (Suchium) moniliferum* (Lamarck),  
582 and associated species on an intertidal sandflat. Res Popul Ecol 36(2):225–236. doi:  
583 10.1007/BF02514939

584 Tamaki A, Ingole B (1993) Distribution of juvenile and adult ghost shrimps, *Callianassa japonica*  
585 Ortmann (Thalassinidea), on an intertidal sandflat: intraspecific facilitation as a possible pattern-  
586 generating factor. J Crustac Biol 13(1):175–183. doi: 10.1163/193724093X00543

587 Tamaki A, Kikuchi T (1983) Spatial arrangement of macrobenthic assemblages on an intertidal sand  
588 flat, Tomioka Bay, west Kyushu. Publ Amakusa Mar Biol Lab Kyushu Univ 7:41–60

589 Tamaki A, Suzukawa K (1991) Co-occurrence of the cirolanid isopod *Eurydice nipponica* Bruce &  
590 Jones and the ghost shrimp *Callianassa japonica* Ortmann on an intertidal sand flat. Ecol Res  
591 6:87–100. doi: 10.1007/BF02353872

592 Tamaki A, Suzukawa K (1997) Life history and zonation dynamics of the cirolanid isopod, *Eurydice*  
593 *nipponica* Bruce & Jones, on an intertidal sandflat in western Kyushu, Japan. Crustac Res  
594 26:83–102. doi: 10.18353/crustacea.26.0\_83

595 Tamaki A, Takeuchi S (2016) Persistence, extinction, and recolonization of an epibenthic gastropod  
596 population on an intertidal sandflat: 35-y contingent history of a key species of the benthic  
597 community in metapopulation and metacommunity contexts. J Shellfish Res 35(4):921–967. doi:  
598 10.2983/035.035.0419

599 Tamaki A, Ueno H (1998) Burrow morphology of two callianassid shrimps, *Callianassa japonica*  
600 Ortmann, 1891 and *Callianassa* sp. (= *C. japonica*: de Man, 1928) (Decapoda: Thalassinidea).

601 Crustac Res 27:28–39. doi: 10.18353/crustacea.27.0\_28

602 Tamaki A, Ingole B, Ikebe K, Muramatsu K, Taka M, Tanaka M (1997) Life history of the ghost  
603 shrimp, *Callinassa japonica* Ortmann (Decapoda: Thalassinidea), on an intertidal sandflat in  
604 western Kyushu, Japan. J Exp Mar Biol Ecol 210(2):223–250. doi: 10.1016/S0022-  
605 0981(96)02709-8

606 Tudhope AW, Scoffin TP (1984) The effects of *Callinassa* bioturbation on the preservation of  
607 carbonate grains in Davies Reef lagoon, Great Barrier Reef, Australia. J Sediment Petrol  
608 54:1091–1096

609 Vader W (1978) Associations between amphipods and echinoderms. Astarte 11:123–134

610 Volkenborn N, Polerecky L, Wetthey DS, DeWitt TH, Woodin SA (2012) Hydraulic activities by  
611 ghost shrimp *Neotrypaea californiensis* induce oxic-anoxic oscillations in sediments. Mar Ecol  
612 Prog Ser 455:141–156. doi: 10.3354/meps09645

613 Wada M, Urakawa T, Tamaki A (2016) Dynamics of bacterial community structure on intertidal  
614 sandflat inhabited by the ghost shrimp *Nihonotrypaea harmandi* (Decapoda: Axiidea:  
615 Callianassidae) in Tomioka Bay, Amakusa, Japan. Gene 576(2):657–666. doi:  
616 10.1016/j.gene.2015.10.017

617 Wardiatno Y, Shimoda K, Koyama K, Tamaki A (2003) Zonation of congeneric callianassid shrimps,  
618 *Nihonotrypaea harmandi* (Bouvier, 1901) and *N. japonica* (Ortmann, 1891) (Decapoda:  
619 Thalassinidea), on intertidal sandflats in the Ariake-Sound estuarine system, Kyushu, Japan.  
620 Benthos Res 58(1):51–73. doi: 10.5179/benthos1996.58.1\_51

621 Woodin SA, Wetthey DS, Volkenborn N (2010) Infaunal hydraulic ecosystem engineers: cast of  
622 characters and impacts. Integr Comp Biol 50(2):176–187. doi: 10.1093/icb/icq031

623 Wynberg RP, Branch GM (1994) Disturbance associated with bait-collection for sandprawns  
624 (*Callinassa kraussi*) and mudprawns (*Upogebia africana*): long-term effects on the biota of

- 625       intertidal sandflats. *J Mar Res* 52(3):523–558. doi: 10.1357/0022240943077019
- 626       Yamada A, Somiya R, Ikeda N, Tamaki A (2017) The complete mitochondrial genome of the
- 627       burrowing ghost shrimp, *Nihonotrypaea harmandi* (Bouvier, 1901), (Crustacea, Decapoda,
- 628       Axiidea, Callianassidae) – a validation of the genus and species classifications. *Mitochondrial*
- 629       DNA B Resour 2(1):238–239. doi: 10.1080/23802359.2017.1318676
- 630       Yamada F, Kobayashi N (2007) Intertidal multiple sand bars in a low-energy environment. *J Waterw*
- 631       Port Coast Ocean Eng 133(5):343–351. doi: 10.1061/(ASCE)0733-950X(2007)133:5(343)
- 632       Yu OH, Soh HY, Suh H-L (2002) Seasonal zonation patterns of benthic amphipods in a sandy shore
- 633       surf zone of Korea. *J Crustac Biol* 22(2):459–466. doi: 10.1163/20021975-99990253
- 634       Zipperle A, Reise K (2005) Freshwater springs on intertidal sand flats cause a switch in dominance
- 635       among polychaete worms. *J Sea Res* 54(2):143–150. doi: 10.1016/j.seares.2005.01.003

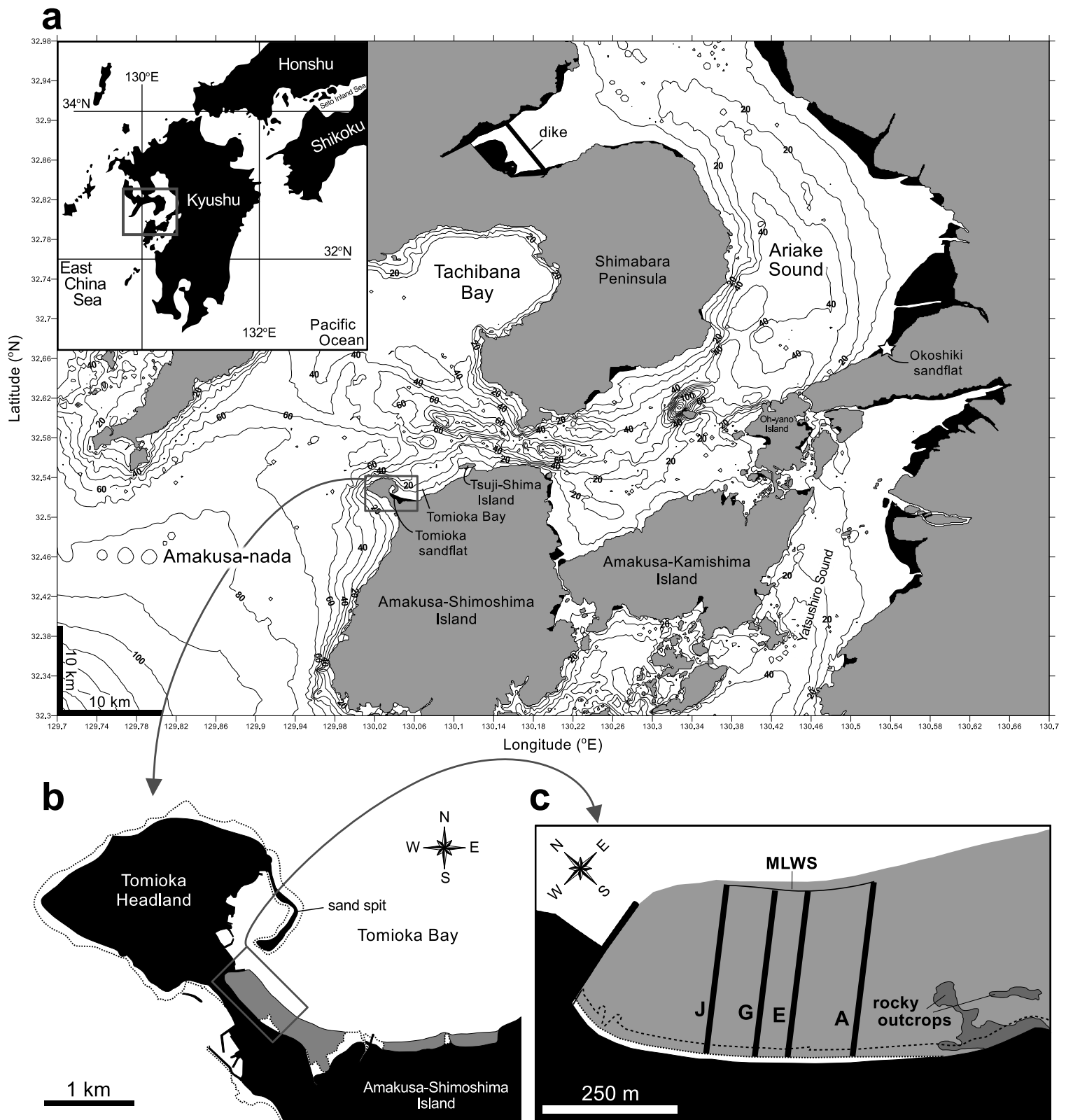


**Fig. 1** **a** Study region and location of the Tomioka (intertidal) sandflat along the shoreline in mid-western Kyushu, Japan. Water-depth isopleths every 10 m were made by contouring (Surfer<sup>®</sup> 8: Golden Software, Inc.) for the point data provided by Hydrographic and Oceanographic Department, Japan Coast Guard. All tidal flats are indicated in black. The Okoshiki sandflat is situated in the middle part of Ariake Sound. **b** Enlarged map of the Tomioka sandflat. The intertidal sandy part and rocky or boulder part are indicated in light gray and white, respectively. **c** Four cross-shore transects (Transects A, E, G, and J) on the monitoring area of the Tomioka sandflat. The sandy part is indicated in light gray. The 10-m wide white-colored zone at the landward edge stands for the hard substrate in 1979–1991, from which the 20-m wide seaward zone down to the broken line was reclaimed during 1991 to 1993. MLWS: mean low water level in spring-tide periods

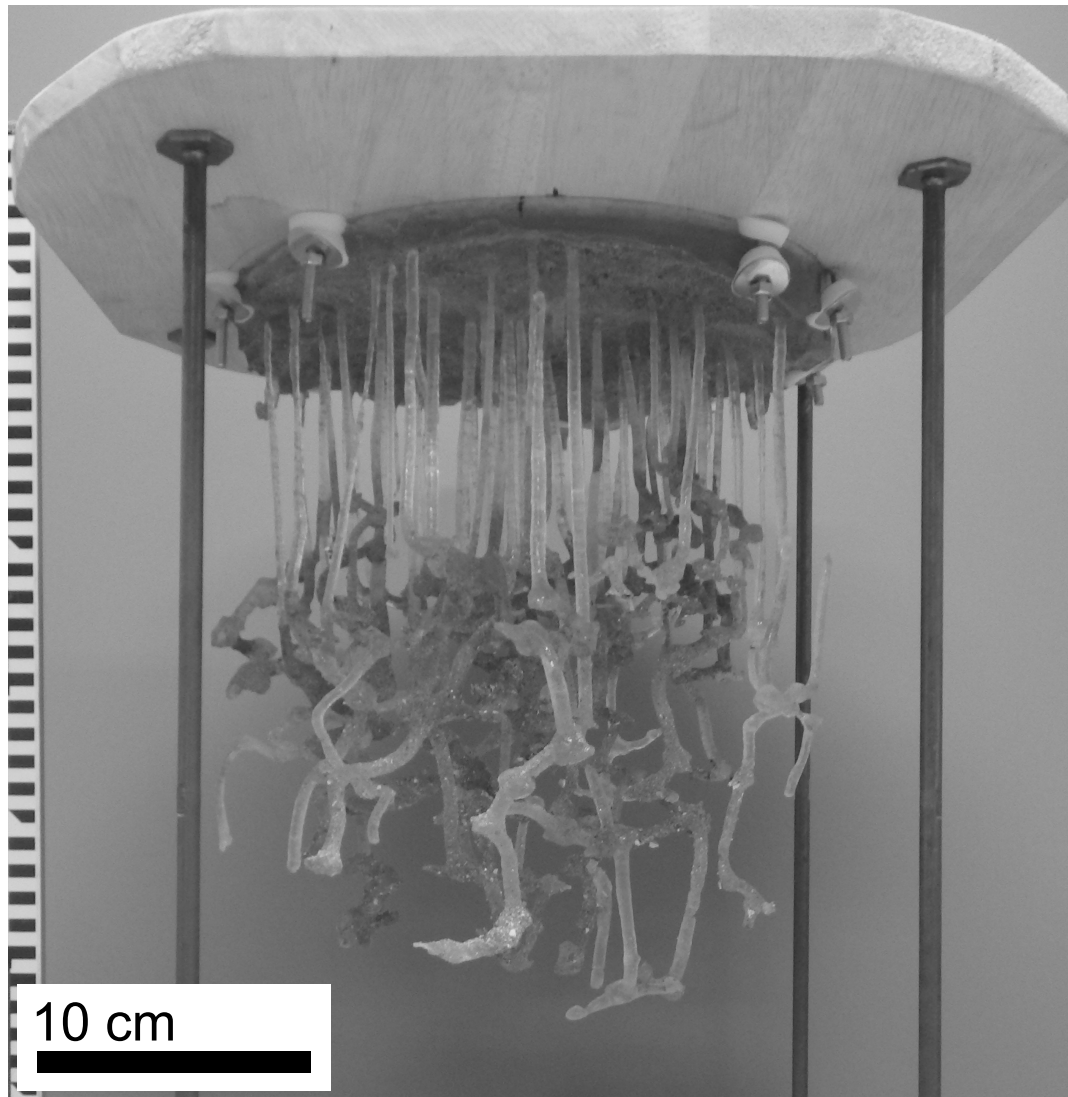


**Fig. 2** Polyester resin casts of burrows of *Nihonotrypaea harmandi* made around the uppermost Tomioka sandflat during 27–28 May 2017

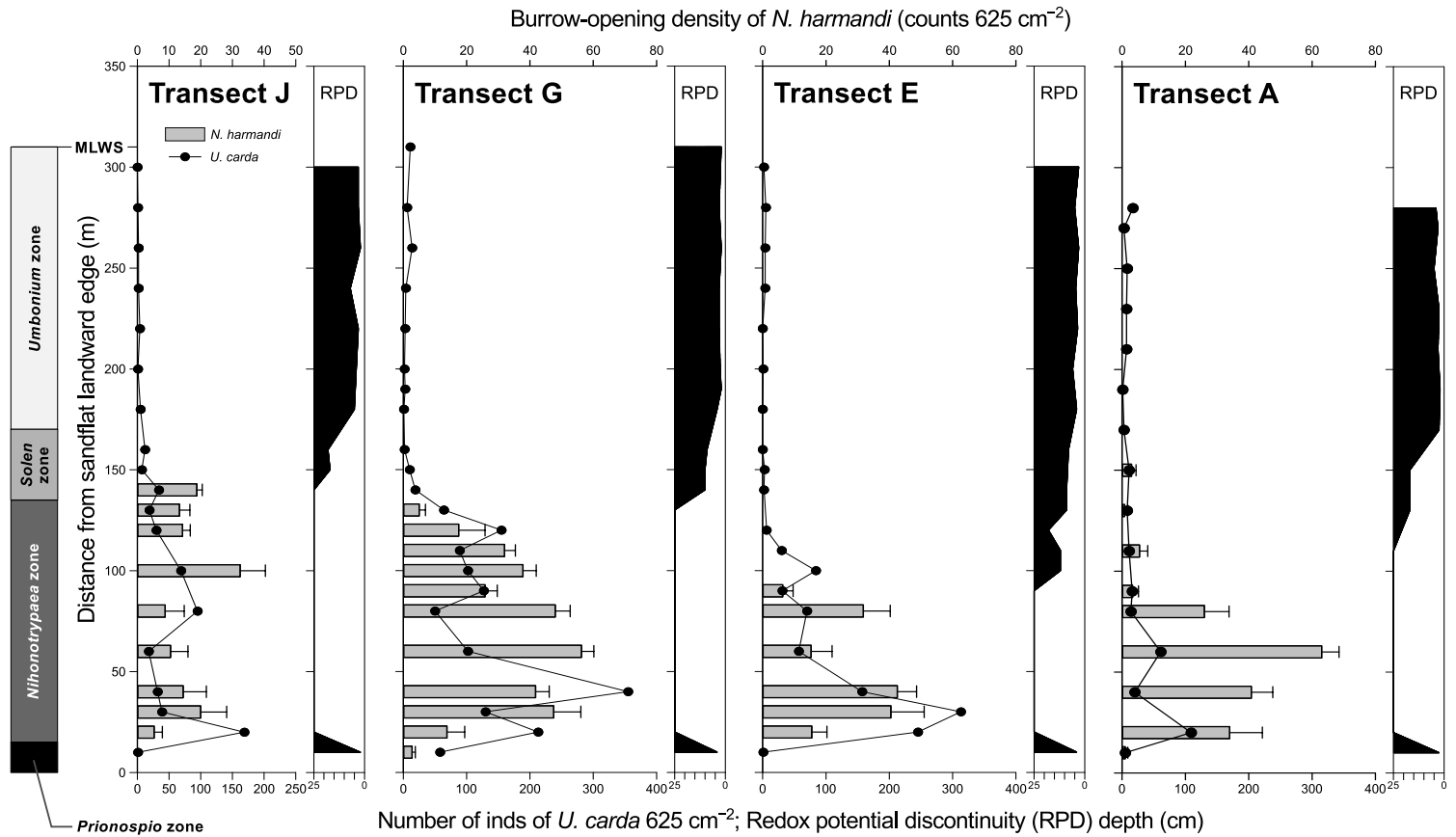


**Fig. 3** Distribution of *Urothoe carda* densities, mean ( $\pm$  SD) surface burrow-opening densities of *Nihonotrypaea harmandi*, and redox potential discontinuity (RPD) depths below the sediment surface along the four cross-shore transects on the Tomioka sandflat (Fig. 1c) on 10–11 August 1980. The numbers of 25-  $\times$  25-cm quadrat frame per station were one for *U. carda* and four for *N. harmandi*. Each RPD depth was determined as the thickness of the brown-colored layer (blank part in the panel) above the gray- or black-colored layers (black part), with the values  $\geq$  25 cm indicated uniformly as 25 cm. The four macrofaunal assemblage zones along Transect G are indicated on the left [designated by genera of representative species (Tamaki 1985)]. MLWS: mean low water level in spring-tide periods. The RPD values on Transect G based on data in Tamaki (1984)

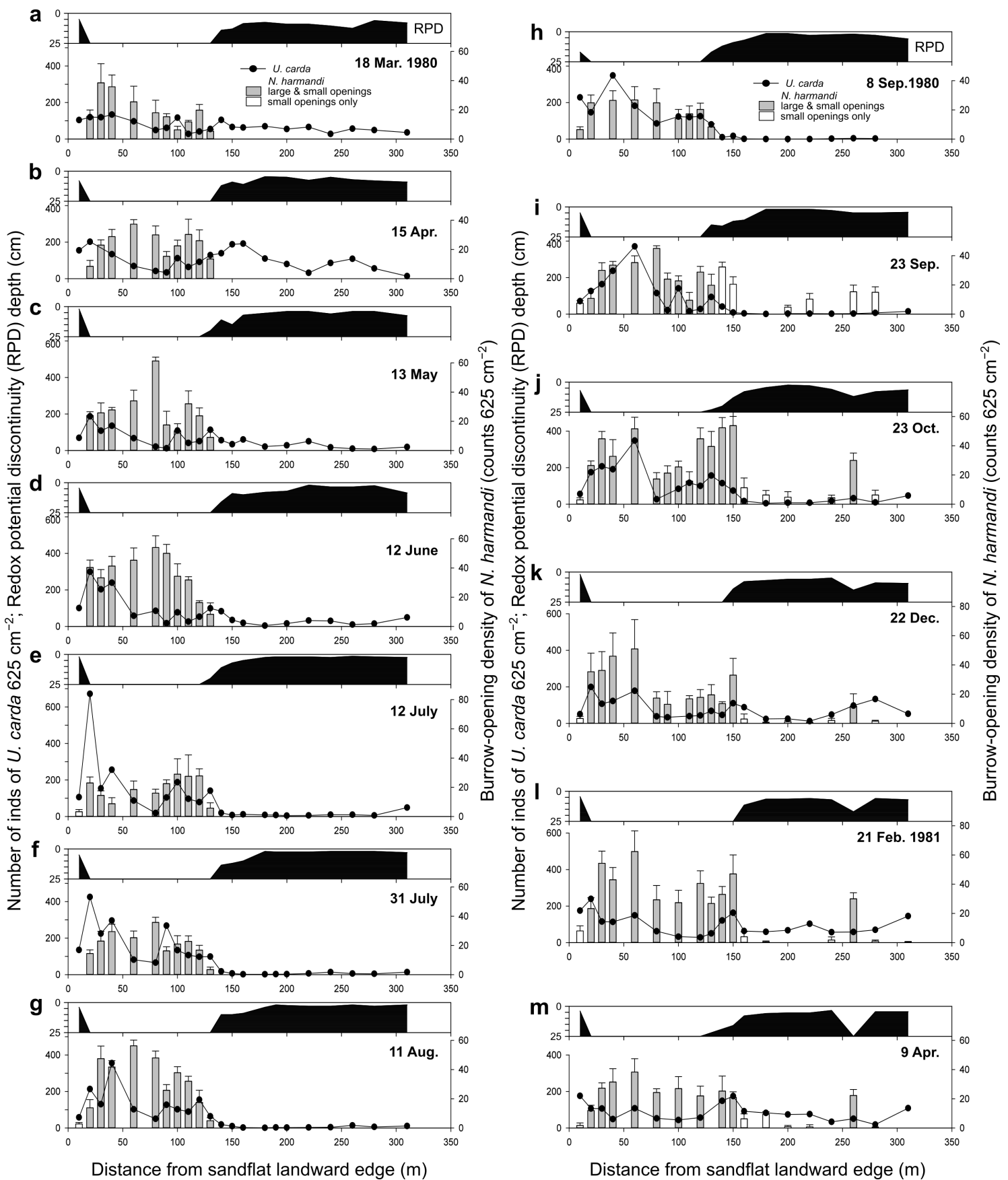


**Fig. 4 a–m** Spatial variations in *Urothoe carda* densities, mean ( $\pm$  SD) surface burrow-opening densities of *Nihonotrypaea harmandi*, and redox potential discontinuity (RPD) depths below the sediment surface along Transect G on the Tomioka sandflat (Fig. 1c) during March 1980 to April 1981. The numbers of 25- $\times$  25-cm quadrat frame per station were one for *U. carda* and four for *N. harmandi*. The stations with both large (3–6-mm  $\phi$ ) and small (1–2-mm  $\phi$ ) burrow openings and those with only small burrow openings are indicated by gray and blank columns, respectively. Each RPD depth was determined as in Fig. 3, based on data in Tamaki (1984)

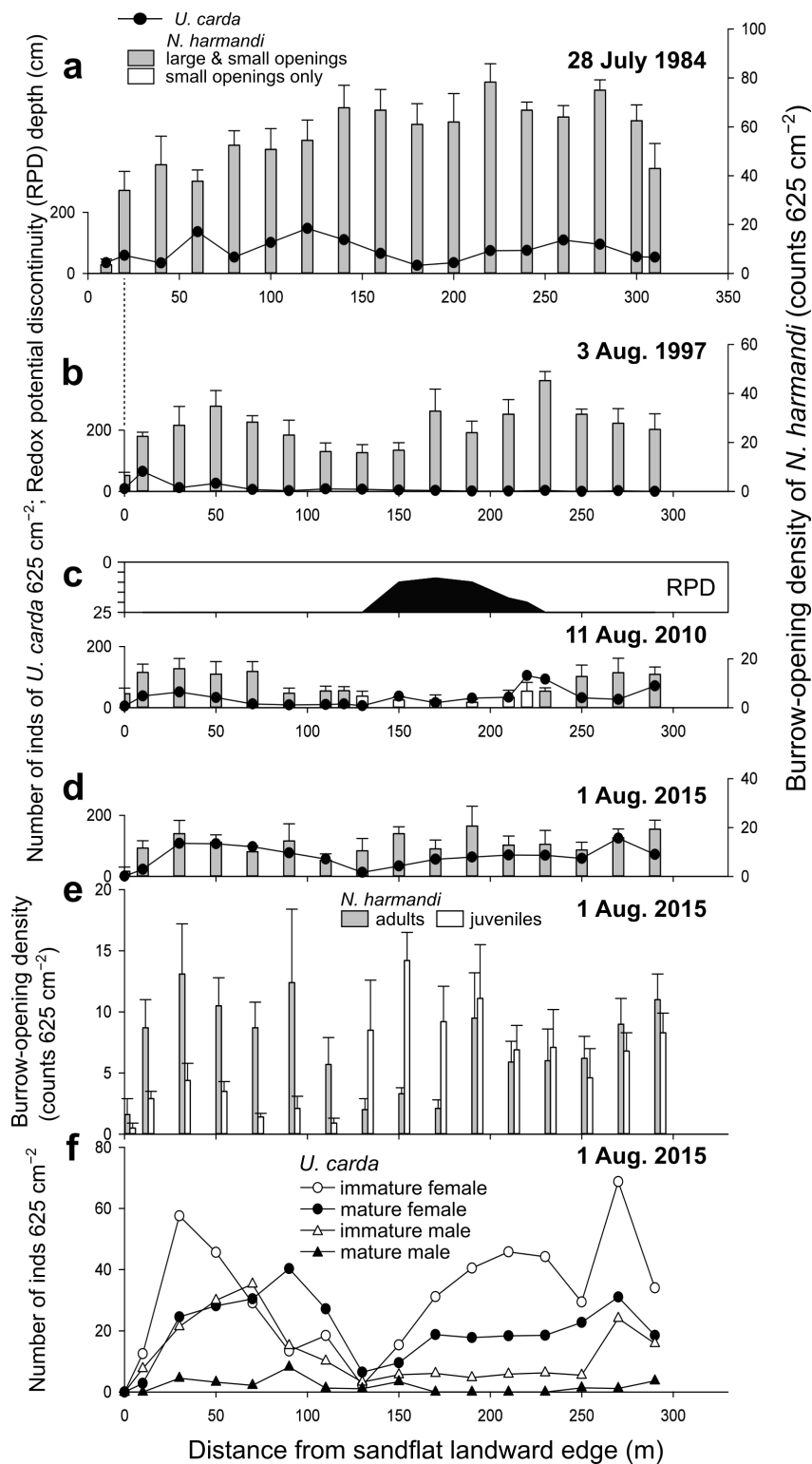


**Fig. 5 a–d** Spatial variations in *Urothoe carda* densities, mean ( $\pm$  SD) surface burrow-opening densities of *Nihonotrypaea harmandi*, and redox potential discontinuity (RPD) depths below the sediment surface along Transect G on the Tomioka sandflat (Fig. 1c) in late July to mid-August in 1984, 1997, 2010, and 2015. Note that the uppermost-shore station in 1997 to 2015 (Stn G-0) was the previous Stn G-20 (1980s). The numbers of 25- $\times$  25-cm quadrat frame per station were one for *U. carda* and four (in 1984) and eight or nine (in 2010 or 2015) for *N. harmandi*. The stations with both large (3–6-mm  $\phi$ ) and small (1–2-mm  $\phi$ ) burrow openings and those with only small burrow openings are indicated by gray and blank columns, respectively. Each RPD depth was determined as in Fig. 3. In 1984, 1997, and 2015, the RPD depths at all stations except for the uppermost-shore station were  $\geq$  25 cm (not shown in a, b, d). **e** Mean ( $\pm$  SD) surface burrow-opening densities of adults and juveniles of *N. harmandi* along Transect G on 1 August 2015, as estimated from the total burrow-opening counts in **d** and the actual proportion of adults and juveniles in the coring tube samples collected on 3 August 2016. **f** Densities of the four groups (mature and immature individuals of each sex) of *U. carda* along Transect G on 1 August 2015. The total number of individuals at each station (**d**) was divided into these groups based on A. Tamaki et al. (unpubl data)

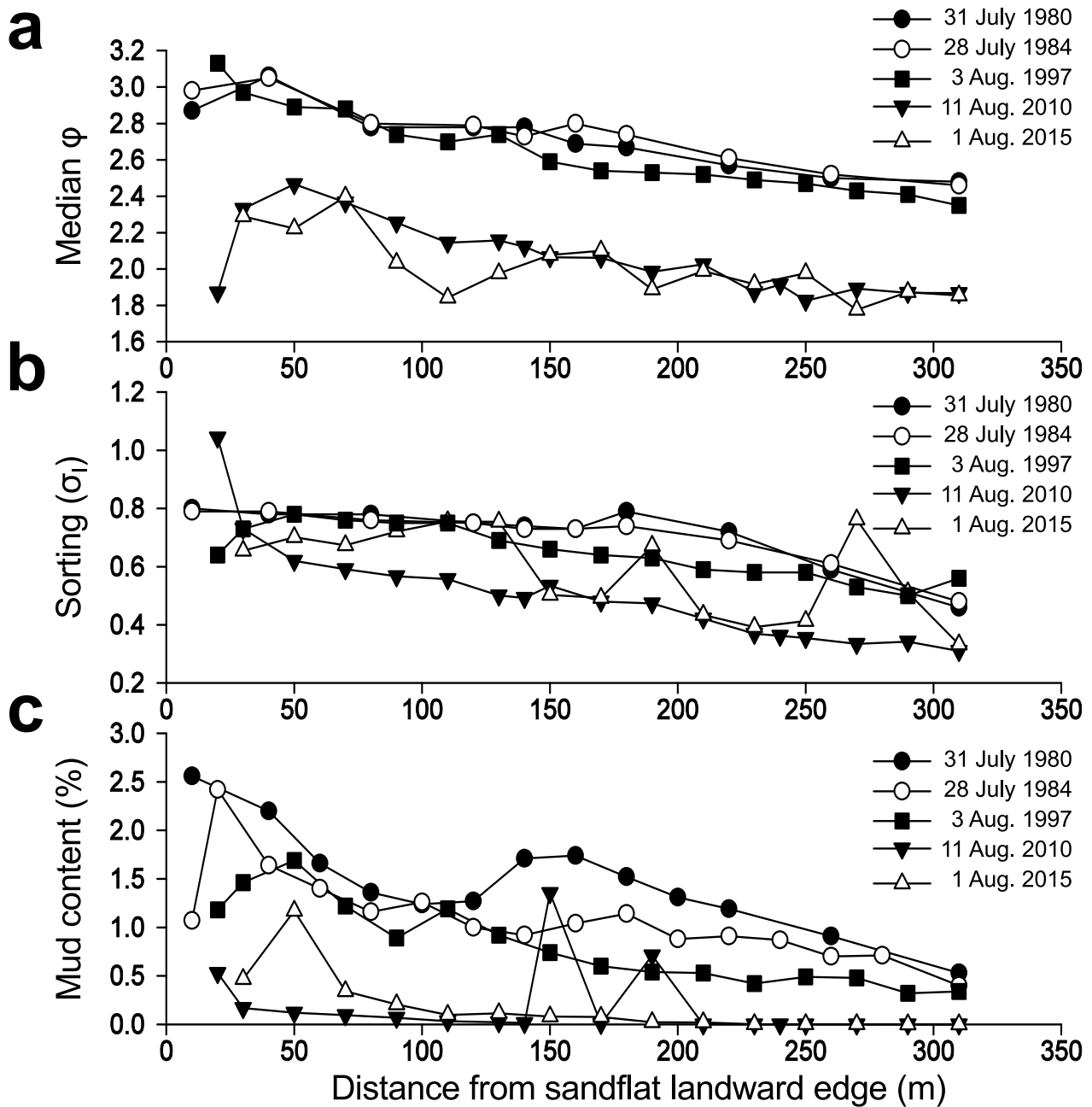


**Fig. 6 a–c** Spatial variations in median  $\phi$ , sorting coefficient ( $\sigma_1$ ; inclusive graphic standard deviation), and mud (= silt-clay) content of the surface 1-cm sediment along Transect G on the Tomioka sandflat in the summers of 1980, 1984, 1997, 2010, and the surface 3-cm sediment in 2015 (sample at Stn G-0 was lost). In 1980, the *Nihonotrypaea harmandi*-inhabited zone was from Stns G-20 to G-130, and from 1984 afterward, the whole transect was occupied by this species. The values in 1980 and 1984 based on data in Tamaki (1984) and Tamaki and Suzukawa (1991)

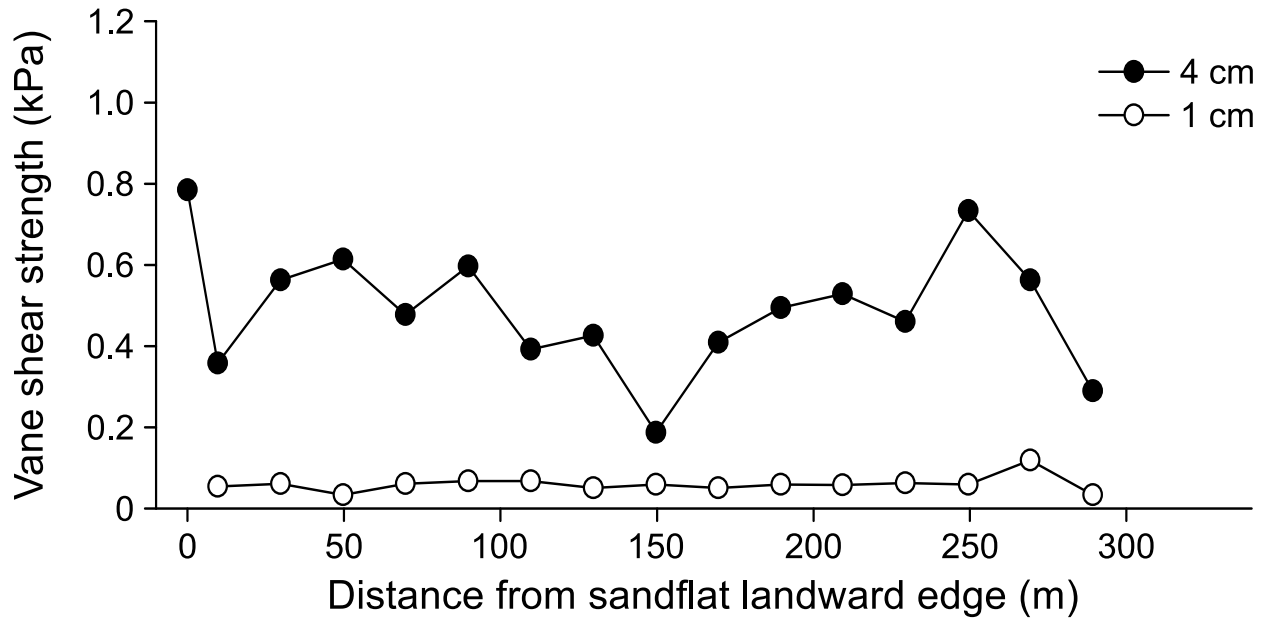


**Fig. 7** Distributions of the vane shear strengths at 4 cm and 1 cm below the sediment surface outside *Nihonotrypaea harmandi* burrow openings along Transect G on the Tomioka sandflat during low tide on 1 August 2015

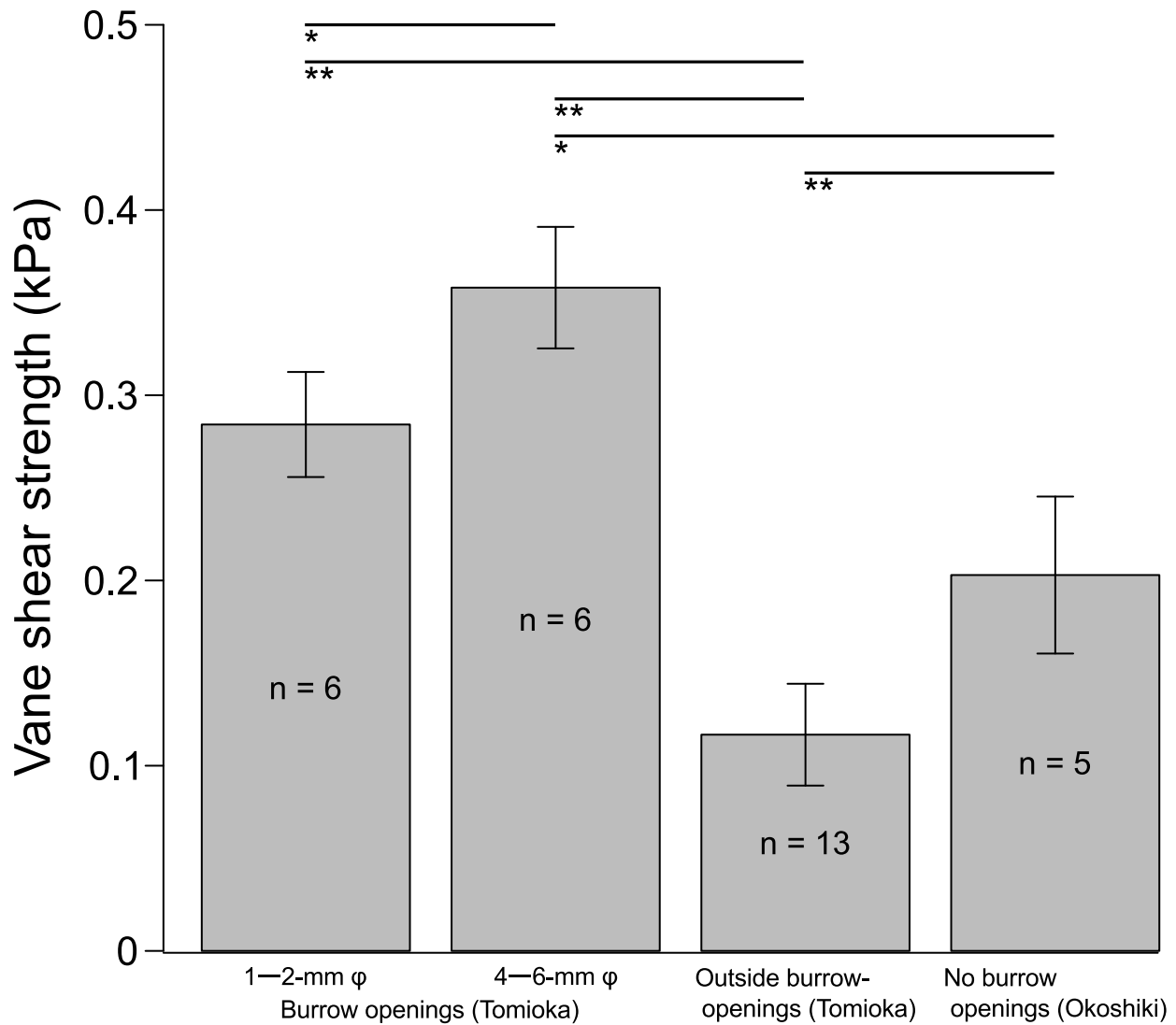


**Fig. 8** Mean ( $\pm$  SD) vane shear strengths at 1 cm below the sediment surface at small *Nihonotrypaea harmandi*-burrow-opening points (1–2-mm  $\phi$ ), large burrow-opening points (4–6-mm  $\phi$ ), outside-burrow-opening points on the Tomioka sandflat during low tide on 1 August 2016 and on trough parts of sand waves with no burrow openings on the Okoshiki sandflat (Fig. 1a) during low tide on 14 June 2010 (from S. Sassa and S. Yang, unpubl data). Each pair with significant difference by Steel-Dwass multiple comparison test is indicated by \* ( $0.01 < P < 0.05$ ) and \*\* ( $0.001 < P < 0.01$ )